Journal of Rock Mechanics and Tunnelling Technology (JRMTT)
31 (2) 2025 pp 121-140

Available online at www.isrmtt.com

Evaluating Tunnel Portal Stability: Insights from the Rishikesh-Karnprayag Railway Project

Khezr Mohammadamini[1]
Hamid Samadi[2,*]

[1]*University of Tehran, Iran*
[2]*Rishikesh-Karnprayag Railway Project, AECOM, India*

**Email: hamid.samadi@aecom.com*

ABSTRACT

The Rishikesh Karnprayag BG Railway Portal 1 of tunnel-11 in India is numerically investigated in this paper. Two-dimensional and three-dimensional models were conducted using FLAC^{3D} software as finite difference method as well as Plaxis 2D software as finite element method to simulate portal excavation and tunnel construction process. Four schemes for tunnel portal stabilization were adopted, including ground improvement, micro pile, bolt mesh shotcrete, and false portal support. The numerical results show that the maximum transverse and longitudinal displacements of surrounding rock are 22 mm. In addition, the study indicated that monitoring had played a guiding role in the study of tunnel stability.

***Keyword*:** Portal slope stability; Portal support; FLAC^{3D}; Plaxis 2D; Monitoring; Inclinometer; Ground subsidence

1. INTRODUCTION

In recent years, many tunnels have been extensively constructed in developing countries for use in subways, highways, railways, material storage, sewage, and water transport, with the aim of improving infrastructure (Fabozzi and Bilotta, 2016). The tunnel entrance is part of the mined section and adjacent to the cut-and-cover approaCh. In which, the buried depth is smaller than two times the tunnel height (Hu et al., 2021). And even more important, tunnel portals are often located in rather weak rock. Also, the ground surface of the tunnel portal section is often inclined to form slopes (Zhang et al., 2013; Goel and Mitra, 2015). Due to the poor rock mass quality at the tunnel entrance, forming the bearing arch is difficult and challenging (Kaya et al., 2017; Goel and Mitra, 2021). Consequently, the tunnel lining at this section is vulnerable and prone to cracking, due to adverse geological factors such as shallow burial depth, asymmetrical loading, and soft, loose surrounding rock (Wu et al., 2015; Chiu et al., 2017). These adverse factors usually work together and present a continuous threat to the tunnel lining, even during the operation stage, especially when the tunnel is disturbed by rainfalls, anthropogenic activities, or earthquakes (Zhen, 2002, Tao et al., 2015; Liu et al., 2018). Structural failure of the entrance section of the tunnel under asymmetrical loads has aroused attention in the engineering field over the past few decades (Zhou et al., 2014). For example, FLAC^{3D} numerical models were used to reveal the cracking and failure

mechanisms of lining for shallow-buried tunnels (Xiao et al., 2014; Xiao et al., 2016) or deep-buried tunnels (Kong et al., 2016) subjected to asymmetrical loads.

Moreover, FLAC^{3D} numerical models were built and conducted to simulate the deformation and displacement behaviors of tunnel lining for asymmetrically loaded tunnels by considering varying transversal gradients, surrounding rock grade, and covering thickness(Lei et al., 2016). Based on theoretical models, a calculation method of asymmetrical rock pressure applied on a super-shallow-buried tunnel was proposed (Zhou et al., 2017).

Additionally, the bearing capacity and the most possible crack areas of the lining were analyzed. Moreover (Simanjuntak et al., 2014; Lei et al., 2015), shaking table model tests were performed to investigate the stress characteristics (Wang et al., 2017), crack coalescence in the process (Wang et al., 2015), and associated mechanism (Xu et al., 2016) of shallow buried asymmetrically loaded tunnels under the influence of earthquakes. Furthermore, the centrifugal model test was applied to explore and examine the stress distribution of lining in an asymmetrically loaded tunnel in bedded rock mass (Liu et al., 2017; He et al., 2022).

Also, studies have been conducted on rock mass issues such as slide, yielding, and cracking of the entrance portal. It was reported that the tunnel portal section linings are most easily damaged under seismic loading (Wang et al., 2001; Geniş, 2010; Shen et al., 2014). And it is interesting to note that most of the earthquake damage mainly occurs near the tunnel portals. In particular, these tunnel portal section linings within the poor geological conditions suffered more severe damage than except tunnel portal section lining (Shen et al., 2014; Xiao et al., 2014). It was investigated the length of reinforcements in the lining of the tunnel portal cross-section with analytical and numerical solutions in seismic conditions; Both analytical solution and numerical results indicated that the seismic fortification length of the tunnel portal section is determined to be not more than 3 three times of tunnel span, and the rock mass rating also has an important essential influence on the tunnel stability of the tunnel portal (Zhang et al., 2013).

This paper examines a railway tunnel entrance in north India to analyze the slope above both escape and main tunnel portals. The stability analysis and displacements of the tunnel entrance and ground subsidence are investigated using FLAC^{3D} and PLAXIS 2D software and compared with monitoring results. Three-dimensional finite difference numerical simulations are conducted to analyze the mechanical characteristics of the tunnel entrance at the entrance section during the excavation of the portal. Corresponding reinforcement measures are proposed to control slope deformation, stabilize surrounding rock masses, and prevent structural damage to the tunnel.

2. PROJECT SPECIFICATION

The 125km new gauge (BG) railway line between Rishikesh and Karanprayag Uttarakhand is a very important project in India. It is proposed to extend the line further to connect with Badrinath and Kedarnath (through future development). Once completed, this project will improve connectivity in Ganga/Alaknanda valley and boost the economy and tourism in Uttarakhand state. Rail Vikas Nigam Ltd (RVNL) is a public sector company under the Ministry of Railways. RVNL has appointed “client” AECOM to carry out the detailed design and project management

consultancy for the construction of tunnels, bridges, and formation works from Ch. 73+489 to 83+899 (10.410km) under Package-6.

Figure 1 - Portal 1 of Tunnel 11, Rishikesh-Karanprayag railway project

2.1 Geological and Rock Mechanical Properties

During the GBR preparation period, the geotechnical investigation data provided by RVNL have been utilized in preparing the geotechnical baseline report for Package 6. Besides this, additional data were also collected during the geological mapping carried out by AECOM in February 2019. The geological plan and L-section for package 6 were done by Geodata.

From the geomorphological point of view, the project area can be divided into two major units: high denudational mountains and river valleys. The Lesser Himalayas (1500-2500 m altitude) are separated from the Siwaliks by the Karol thrust (the main boundary fault). Tunnel-11 of the Rishikesh-Karanprayag project, located in the Jaunsar group, which is part of the outer lesser Himalayan zone, is characterised by superimposed thrust sheets [Nappe Tectonics (NPT)] where the Garhwal group overlies the Jaunsar group. Portal-1 of Tunnel 11 in Srinagar is located in the river terrace material, which is loosely bounded and consists of RBMs in sub-round sizes (Fig. 1), mixed with a sand and clay matrix. Intermittent outcrops of the Chandpur formation phyllite are also exposed near the highly weathered portal site.

River-bearing material (RBMs) has been observed at portal-1 of tunnel-11 (T-11) due to the presence of river terraces of the old layer (Fig. 2). The discontinuities recorded from the bedrock outcrops exposed between portals 1 and the middle portions have been mapped together. The bedrock in this area is traversed by three sets of discontinuities (S1, S2, and S3) along with some random joints (Table 1). Figure 3 shows the plotting of discontinuities in equal area projection. Variation in the attitude of the joint sets may be expected locally around the area due to local fold and faults.

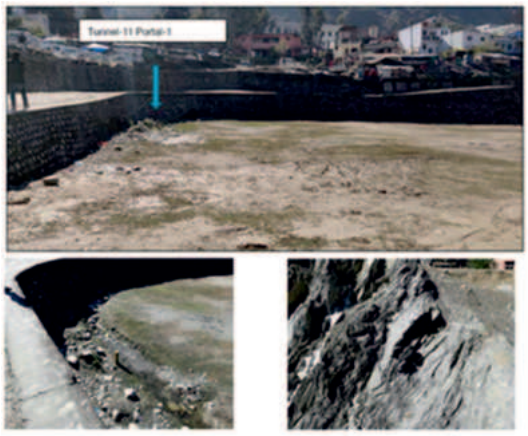

Figure 2 - Portal 1 of T11 location and exposed rock

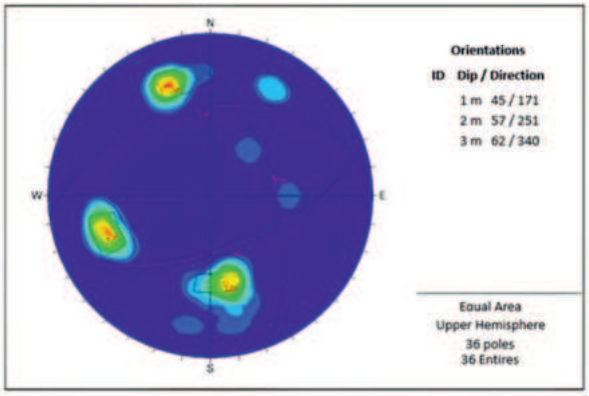

Figure 3 - Plot of 36 poles of discontinuities in the upper hemisphere of equal area projection along the portal 1 (T11)

Table 1 - Discontinuities properties along the portal-1 area of T-11

Portal-1 of T 11 (Ch.73+800 to 74+600 km)			
Discontinuity	S1	S2	S3
Dip/Direction	40-50°/160-190°	50-65°/240-260°	55-70°/335-355°
Roughness	RP-RU	RU-RP	RU-RP
Spacing	Closely spaced (5cm-25cm)	Close to wide (15cm-200cm)	Close to wide (30cm-200cm)
Aperture	Aperture opening (5mm-1cm)	Aperture opening (2mm-5mm)	Aperture opening (2mm-5mm)
Filling	Clay to none	None to clay	Clay to none
Persistence	>10m	>3m	>2m

Notations: RP- Rough planar; RU – Rough undulating

Portal 1 of T 11 is located at Ch. 73+800 km. The slope at the portal site is mild (10 to 25°), with an overburden of 18m. Portal-1 of T11 is situated on the river terrace deposits, which comprises rounded to sub-rounded boulders and cobblestones of phyllites and quartzites intermixed with silty sand and clay. Bedrock intercepted deep at this location is thinly foliated, weak to medium strong, moderately to highly weathered, and grey to buff-coloured phyllites. A borehole (BH-98) has been drilled to optimize the portal location. The longitudinal section along portal 1, T11 is shown in Fig. 4. Figure 5 shows the plan and elevation of cross-section of portal 1 of T11, whereas the photograph of the portal is shown in Figure 6.

Terrace and slide material at the crown level between Ch. 73+800km and Ch. 73+960km includes the portal-1 of T11 in the deep river terrace material, followed by the fractured and weathered phyllites. The depth of terrace material varies between 25m and 56m. This kind of material at the tunnel location may lead to crown failure due to the heterogeneous nature of the ground and water ingress. To effectively control these risks, it is imperative to implement appropriate measures, such as stiff support systems, grout injection, and effective drainage solutions.

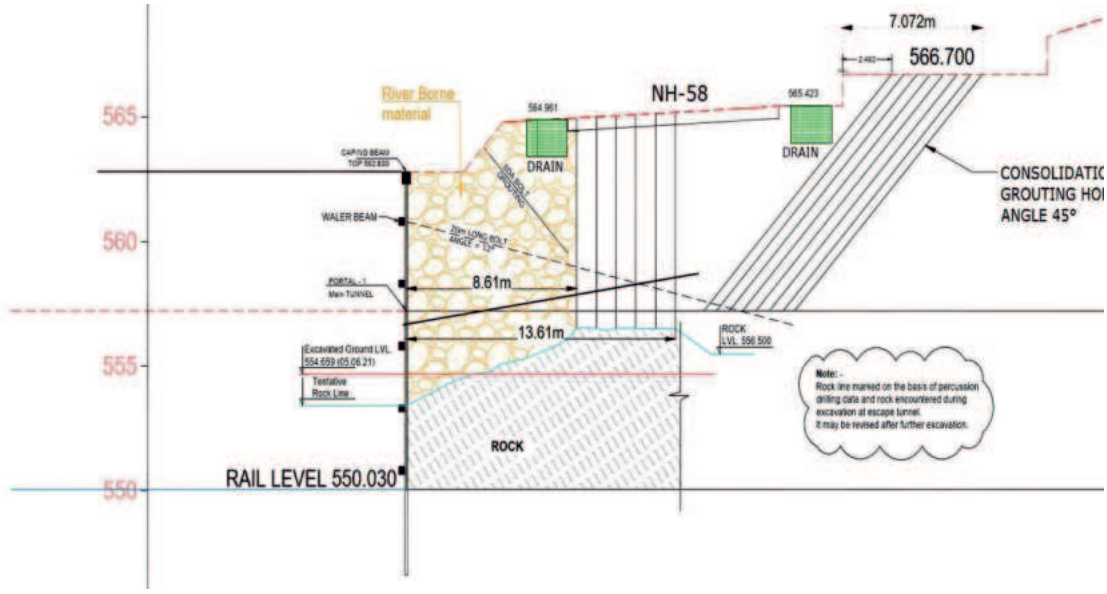

Figure 4 - Longitudinal section of portal 1, T11

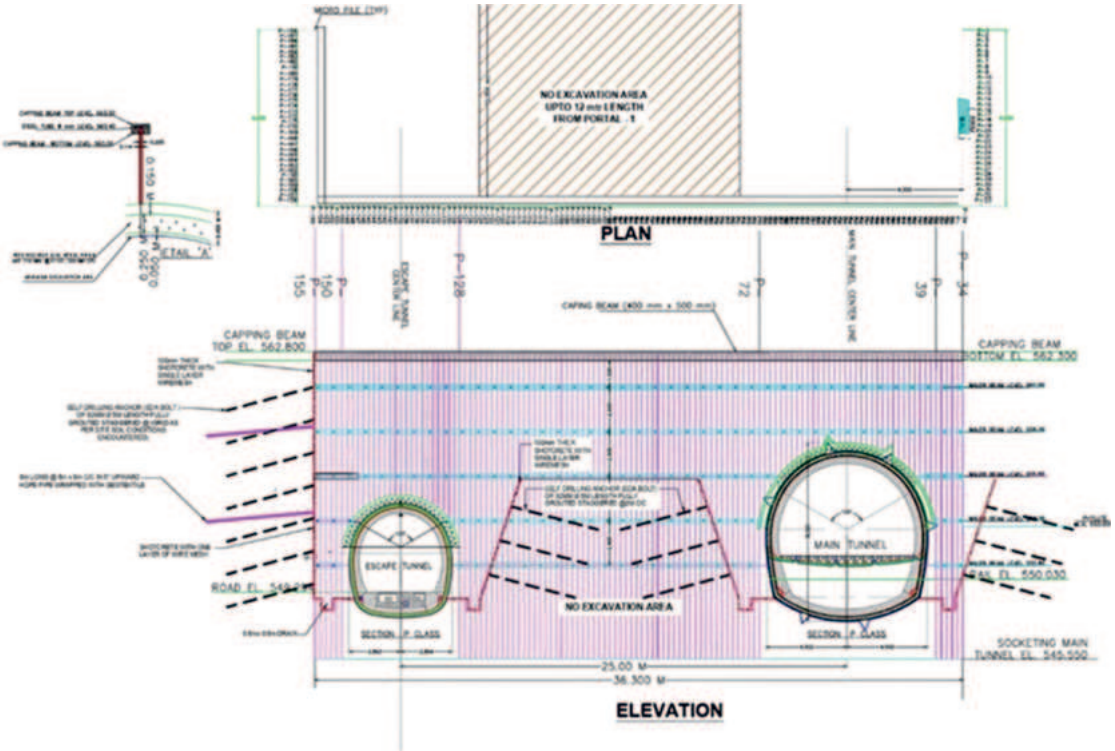

Figure 5 – Plan and elevation of escape and main T11 at portal 1

3. NUMERICAL MODELLING

The tunnel portal is a three-dimensional problem and requires three-dimensional numerical calculations to identify the behaviour and response of the ground. Idealized numerical modelling provides significant assistance in identifying the ground response and its reactions in a short time. In this paper, Plaxis 2D software was initially used to identify the ground behaviour fully. Then,

FLAC 3D software was used with full details to compare with the behaviour data. Geometry of the numerical models in Plaxis 2D and FLAC^{3D} is shown in Figures 7 and 8 respectively.

Figure 6 – Photograph of escape and main T11 at portal 1

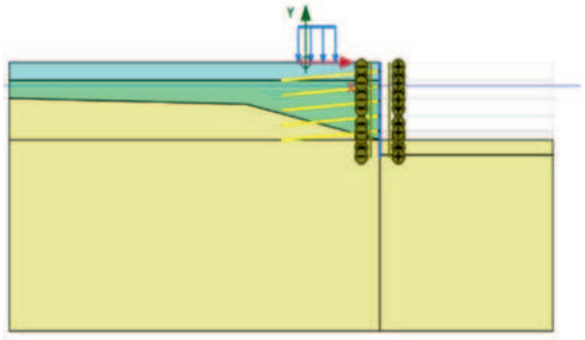

Figure 7 - Geometry of numerical model in Plaxis 2D

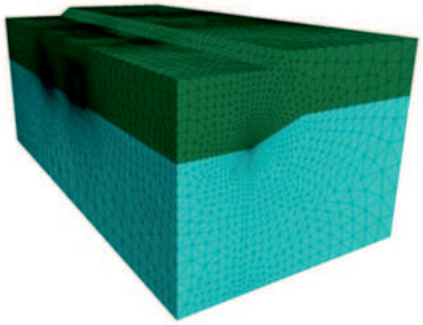

Figure 8 - Geometry of numerical model in FLAC3D

The limitations of this numerical analysis study include the following three points:

- The Mohr-Coulomb constitutive model was used.
- Stresses were calculated automatically by the software.
- The tunnel entrance excavation was modelled in 5 stages, while in reality, it occurred in 8 stages.

In addition to, considering that weathering is quite intense in the Himalayas, drainage systems measuring 5 × 5 m with a diameter of 54 mm and spaced 3m × 3m apart have been utilized to prevent surface weathering. However, as a general hypothesis of this study, the long-term effects of weathering have not been taken into account.

The simulation is conducted in following seven steps.

- Creating initial stresses.
- Balancing the model.
- Installing micro-piles.
- Improving ground conditions around the tunnel.
- Applying surcharge loading.
- Sequential excavation of the tunnel portal and its stabilization.
- Constructing a false portal and backfilling over it.

The surcharge loading was estimated to be 20kN/m. The tunnel portal was excavated in five steps in a sequential excavation. In each stage, a portion of the trench excavation was carried out at a specific height. At each stage, after the excavation of soil, Waller beams and rock bolts will be installed, and shotcrete will be applied to the wall.

As a starting point for this analysis, the ratio of horizontal to vertical stresses is equivalent to Jaky equation. According to the ICE value, elastoplastic behaviour was suggested, and Mohr-Coulomb criterion was considered for the modelling of soil and rock. The ground class at the location of portal 1 is classified as GT6 due to the presence of soil and overburden. The material properties of soil strata and overburden mass comprising of pebbles and boulders of phyllites and quartzites are listed in Table 2. The micro-pile wall is modelled as a pile element with design properties as mentioned in Table 3.

Table 2 - Material design properties of soil and overburden mass

Parameters / Ground type	Saturated Unit Weight (kN/m^3)	Dry Unit Weight (kN/m^3)	Cohesion (kPa)	Friction Angle (°)	Youngs Modulus E (MPa)
Soil Strata	20	18	10	28	10
Overburden Mass	22	20	50	30	50

Table 3 - Design parameters of micro-pile

Properties	Design Values (Plaxis 2D)	Design Values ($FLAC^{3D}$)
Normal stiffness, EA (kN/m)	5.580E6	-
Flexural rigidity, EI (kNm^2/m)	2690	-
Unit weight, w (kN/m/m)	2.100	-
Poison ratio	0.15	0.15
Young's modulus (GPa)	-	200
Outer diameter (mm)	114	114
Thickness (mm)	8	8
Normal coupling spring stiffness (GPa)	-	2.34
Shear coupling spring stiffness (GPa)	-	97.4

Based on the geological conditions, structure fractures, and geotechnical parameters of the tunnel route, it was divided into seven ground types. To optimize and select the most suitable maintenance system, seven support systems were proposed for the route. Details of all the ground types are not covered in the paper. Portal 1, T11 has been classified under P support class and discussed here. The properties of rock bolts and shotcrete in P support class are given in Table 4 and used in the numerical analysis of portal 1, T11.

4. DESIGN OF PORTAL SLOPES

The following stages were followed to simulate the excavation process during numerical analysis:

- Stage 1: Initial ground conditions.
- Stage 2: Reset displacements to zero and activate surcharge load.
- Stage 3: Activate the plate element and interfaces representing the micro-pile installation.

- Stage 4: Reset displacements to zero, excavate 3m of the soil, and activate the 1st layer of anchors at a depth of 1.5m.
- Stage 5: Excavate up to 6m of the soil; activate the 2nd layer of anchors at 2.5m spacing c/c from the first layer of the anchor.
- Stage 6: Excavate up to 9m depth; activate the 3rd layer of Anchors at 2.5m spacing c/c from the second layer of the anchor.
- Stage 7: Excavate up to 12m depth; activate the 4th layer of Anchors at 2.5m spacing c/c from the third layer of the anchor.
- Stage 8: Excavate up to 13m depth; activate the 5th layer of Anchors at 2.5m spacing c/c from the fourth layer of the anchor.
- Stage 9: Create false portals and backfilling.

Different stages models are shown in Figs. 9a to 9d.

Table 4 - Properties of rock bolts and shotcrete of support class P

Anchor/ Bolt/Shotcrete Properties	*Value*
Youngs modulus, E_s (GPa)	200
Friction angle, ϕ (degree)	32
Bolt length, L_b (mm)	6000
Transverse bolt spacing, S_t (mm)	1000
Longitudinal bolt spacing, S_l (mm)	1000
Tensile capacity, T_b (N)	200000
Shotcrete	
Youngs modulus, E_c (GPa)	30
Tunnel radius, R_0 (mm)	3000
Shotcrete thickness t_c (mm)	250
Poisson's ratio, υ	0.2
Stiffness of bolt	0.016362
Stress in bolt (N/mm^2)	0.2
Stiffness of concrete	0.907513
Stress in concrete (N/mm^2)	2.395833
SDA Bolt diameter (mm)	32

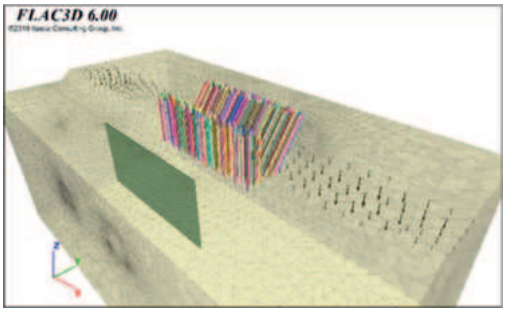

a) Ground improvement and traffic load

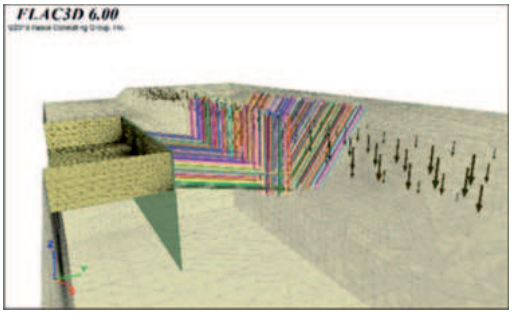

b) First level of excavation

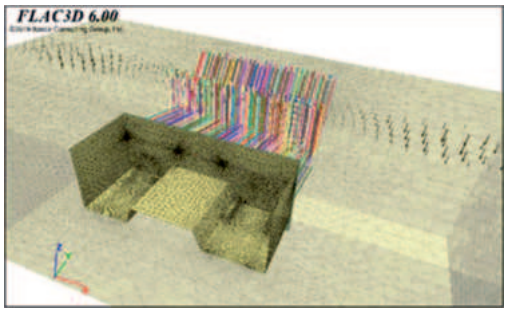

c) Final level of excavation

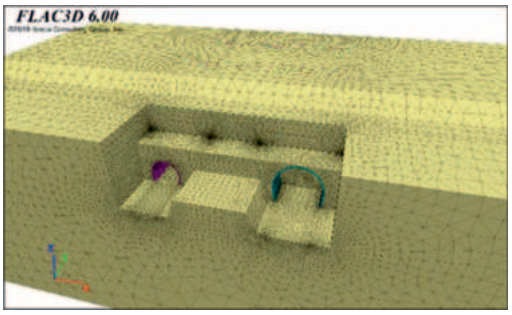

d) Install false portals and filling

Figure 9 - Steps of simulating improvement and excavation

5. RESULTS OF NUMERICAL ANALYSIS AND DISCUSSION

5.1 Micro-Pile Behaviour

The profiles of displacements, axial forces, shear forces, and bending moments in the micro-pile are shown in Figure 10 to 11. According to Fig. 10Figure 10(a), the maximum displacement in micro-piles is determined to be 22 mm. This value occurred only at the location of the main, in the absence of the beam and anchor.

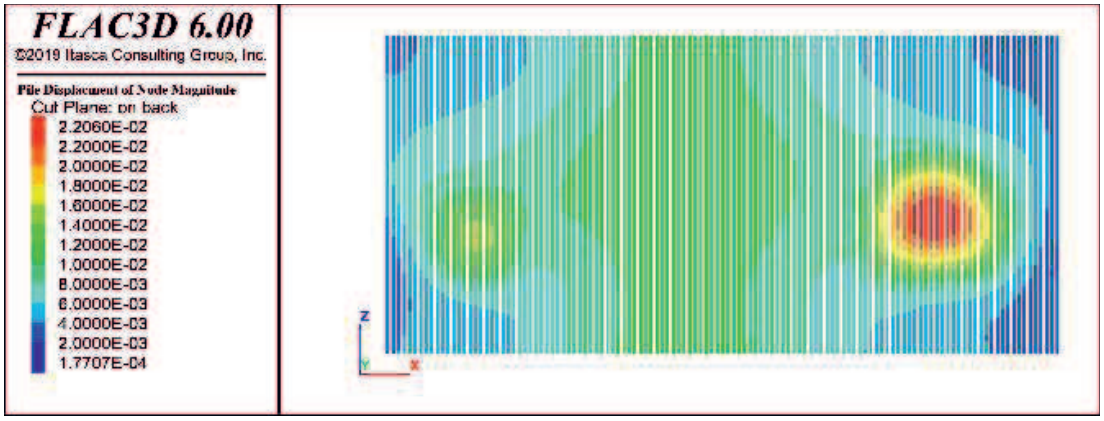

a) magnitude displacement of micro-pile

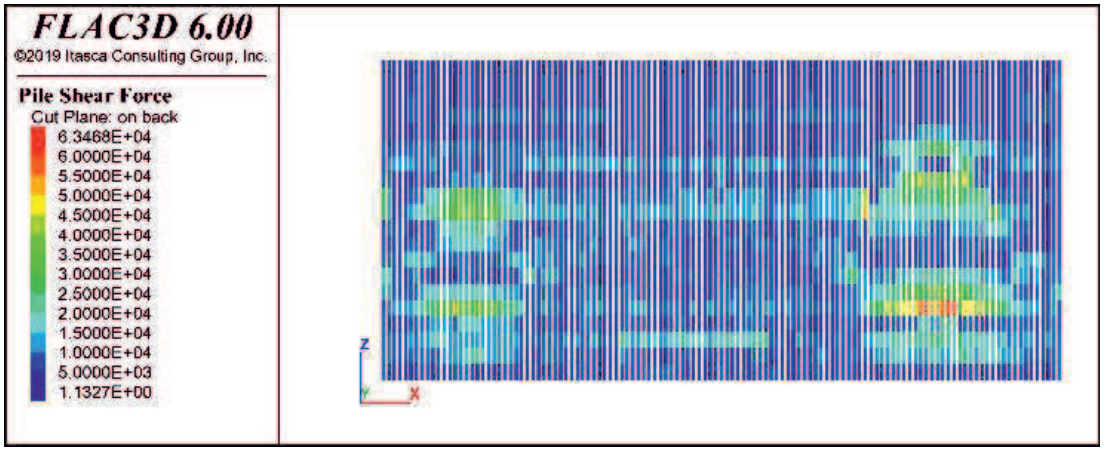

b) Shear force of micro-pile

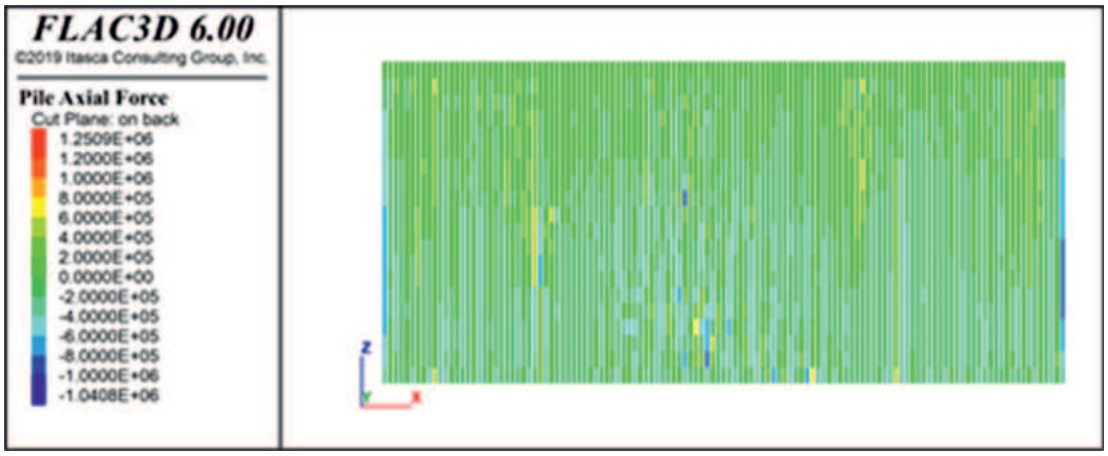

c) axial force of micro-pile

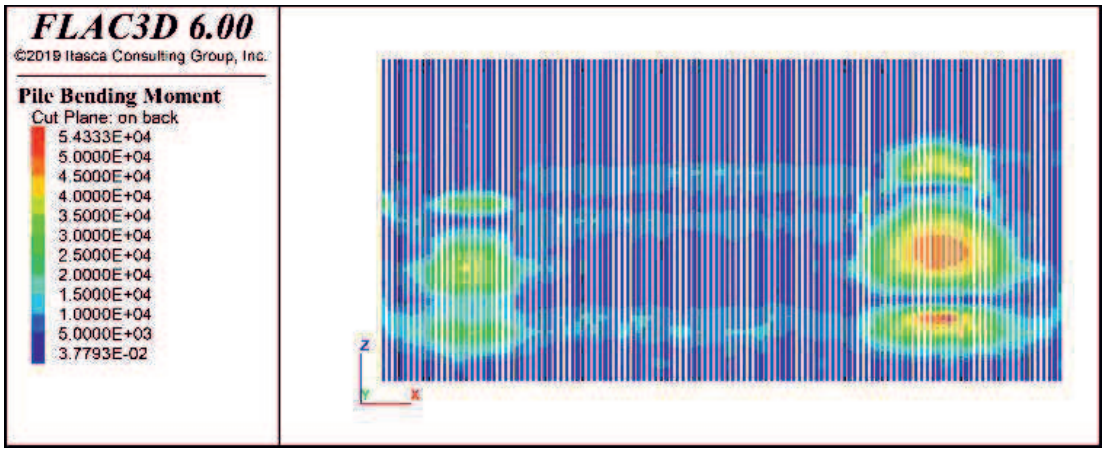

d) bending moment of micro-pile

Figure 10 - Results of micro-pile from FLAC3D analysis

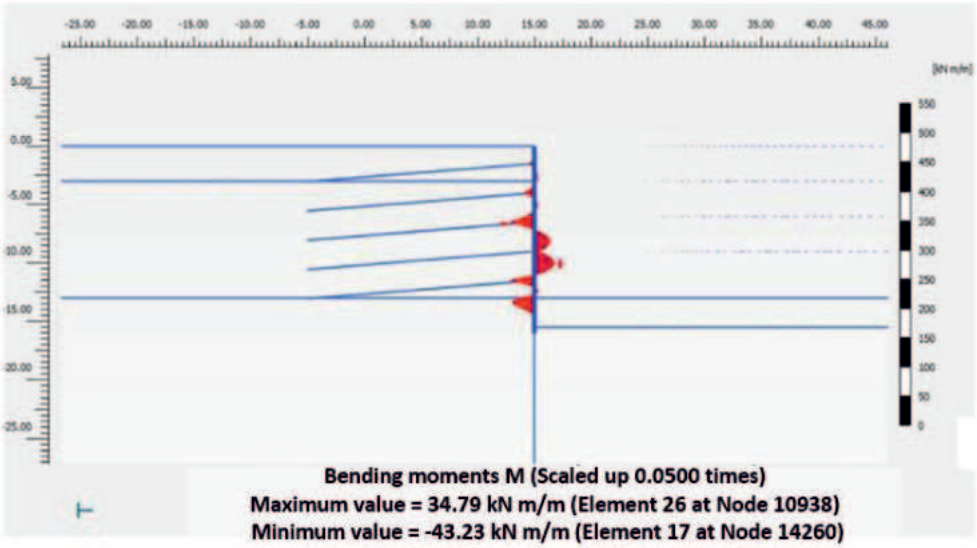

Figure 11 - Bending moment of micro-pile conducted by Plaxis 2D

The maximum bending moment in the micro-pile calculated by Plaxis2D and FLAC^{3D} ware 45.23kN m/m and 54.33kN m/m, respectively. The difference in values is because of the absence of the Waller beams in the Plaxis 2D and assuming the anchors in elongation. However, the

anchors have not been installed in the tunnels, and the intensity of the difference is great only at the tunnel locations. The bending moment is sufficient for the design.

5.2 Anchors Behaviour

The anchors are designed as plate elements in Plaxis 2D and as cable elements in FLAC^{3D}. The distance between the anchors is 0.9m c/c, and the maximum force of the anchor is equal to the force obtained from the model. Maximum axial force in the anchors calculated in Plaxis 2D (bottom level) and FLAC^{3D} (side of main tunnel area) was 193 kN and 182.17kN, respectively. The difference in values is that anchors are assumed to be elongated in Plaxis 2D software. It can be seen that the anchor is stable and does not fail (Figure 12).

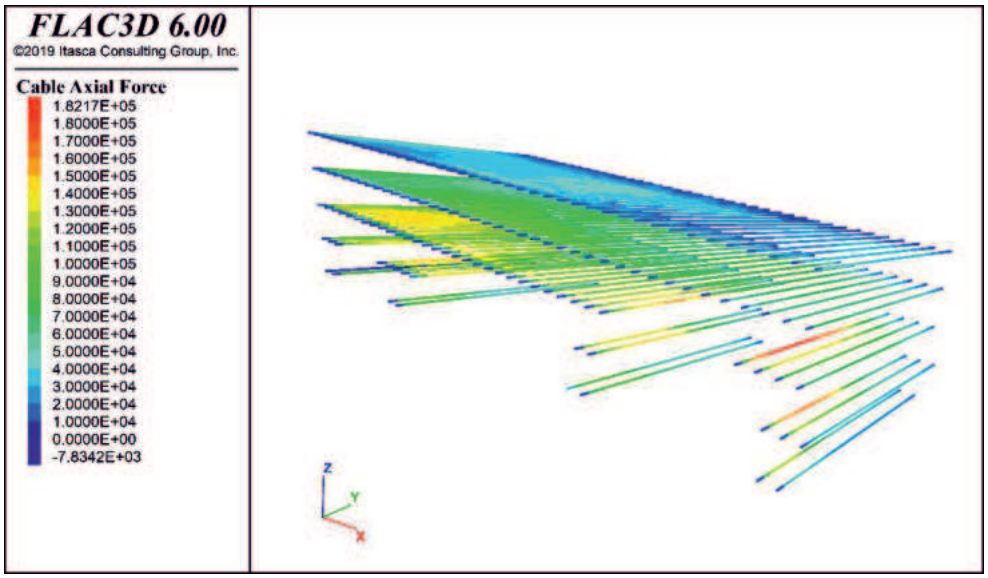

a) Axial force in anchor bolts in FLAC3D

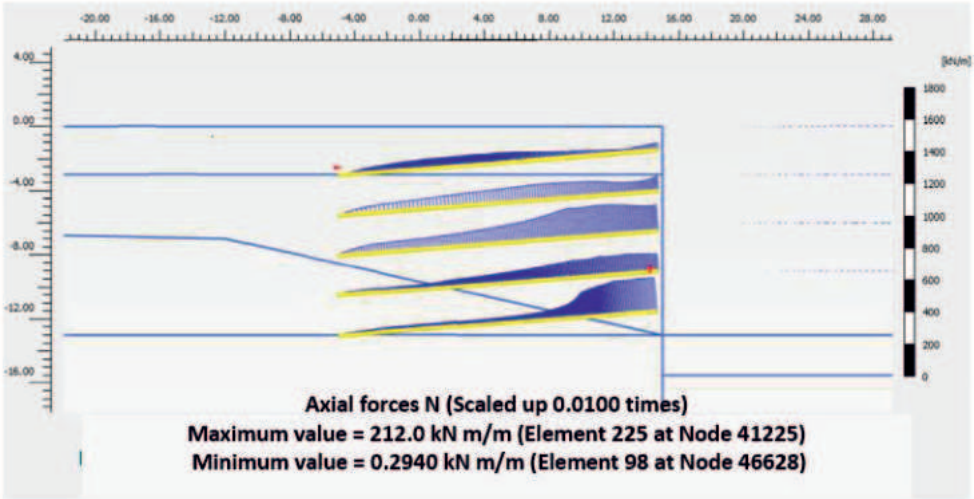

b) Axial force in anchor bolts in Plaxis 2D

Figure 12 - Axial force in anchor bolts

5.3 Ground Deformation

Maximum ground deformation computed in Plaxis 2D and FLAC^{3D} was 61mm and 131mm, respectively. However, the maximum displacement in the direction of the tunnel axis in Plaxis 2D and FLAC^{3D} is equal to 40 mm and 22 mm, respectively. Also, the maximum displacement in the transverse of the tunnel axis in FLAC^{3D} is equal to 22 mm, as shown in Figure 13 (b). FLAC^{3D} values are closer to the actual observed/monitored deformation values. The purpose of using Plaxis 2D was for preliminary design and sensitivity analysis to save time. The FLAC^{3D} output was used as the required output for comparison with the observed/monitored deformation values.

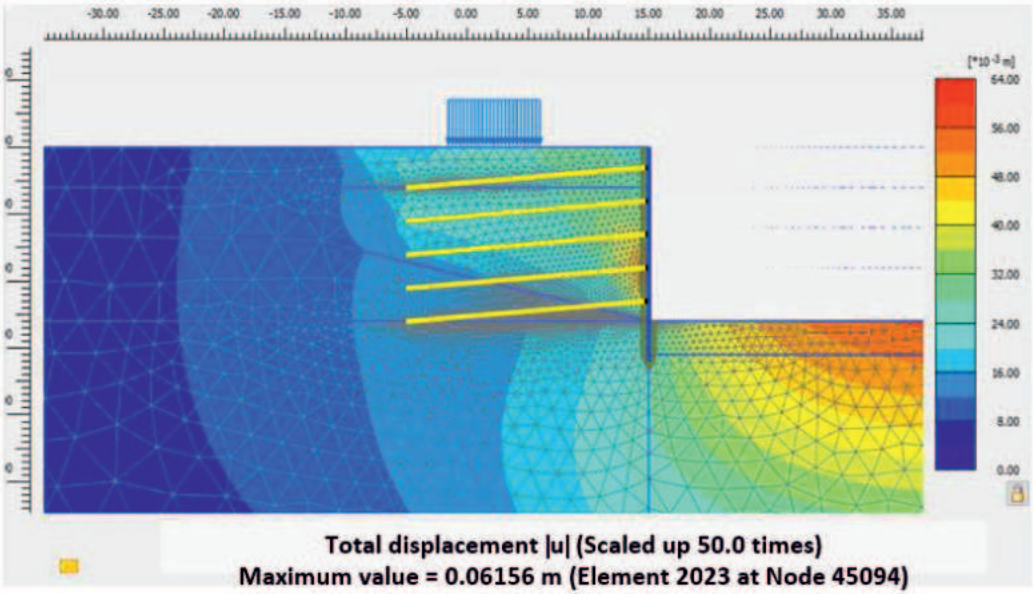

(a)

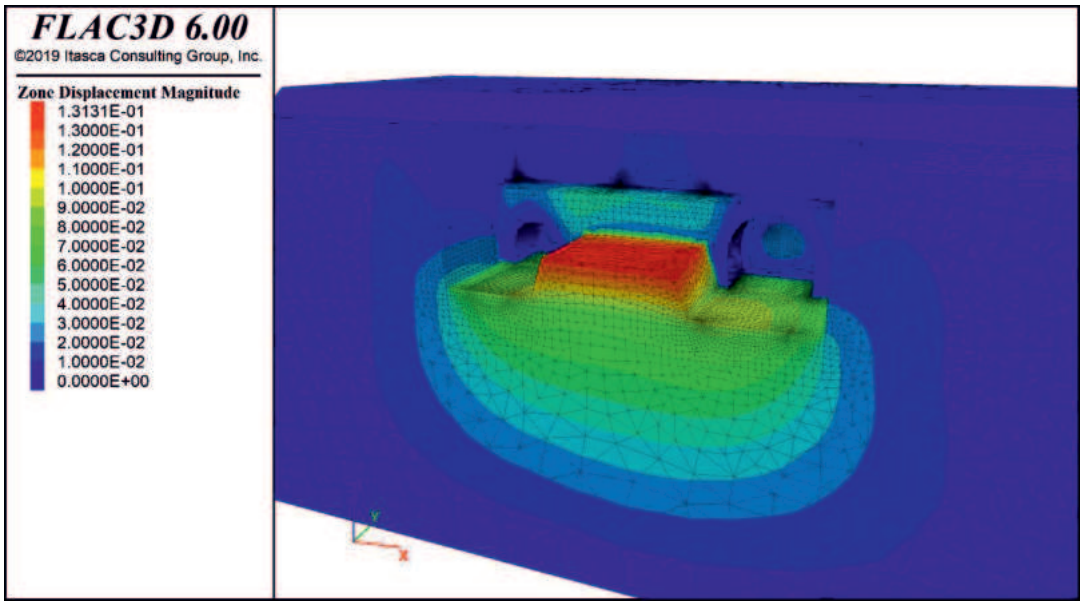

(b)

Figure 13 - Deformation contour, a) Plaxis 2D, b) FLAC^{3D}

5.4 Displacements in Tunnel

The displacement in the direction of the tunnel axis in the final stage of excavation was calculated at 13mm, as shown in Figure (a), and on the final of filling and installing false portals, it was calculated at 22mm, as shown Fig. 14(b). Also, the maximum displacement in the escape tunnel was calculated at 13mm (as indicated in Fig. 14(c)), the maximum displacement in the main tunnel was determined at 21mm (as illustrated in Fig. 14(d)).

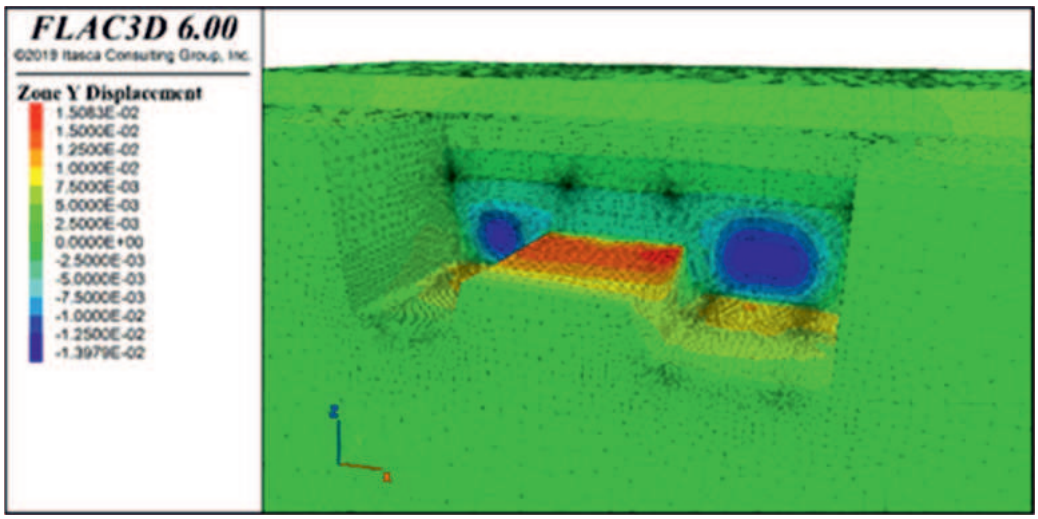

a)

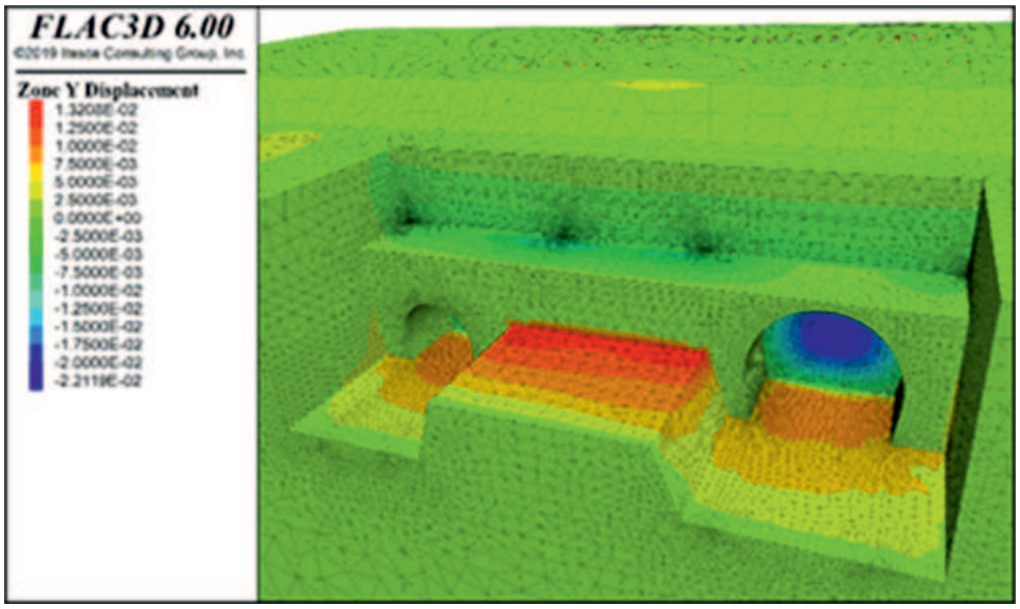

b)

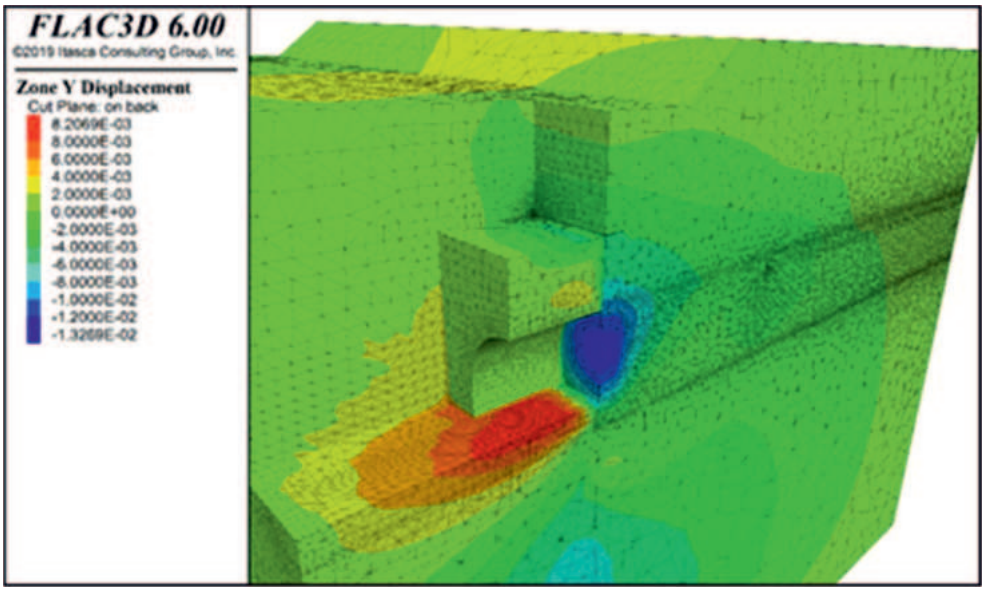

c)

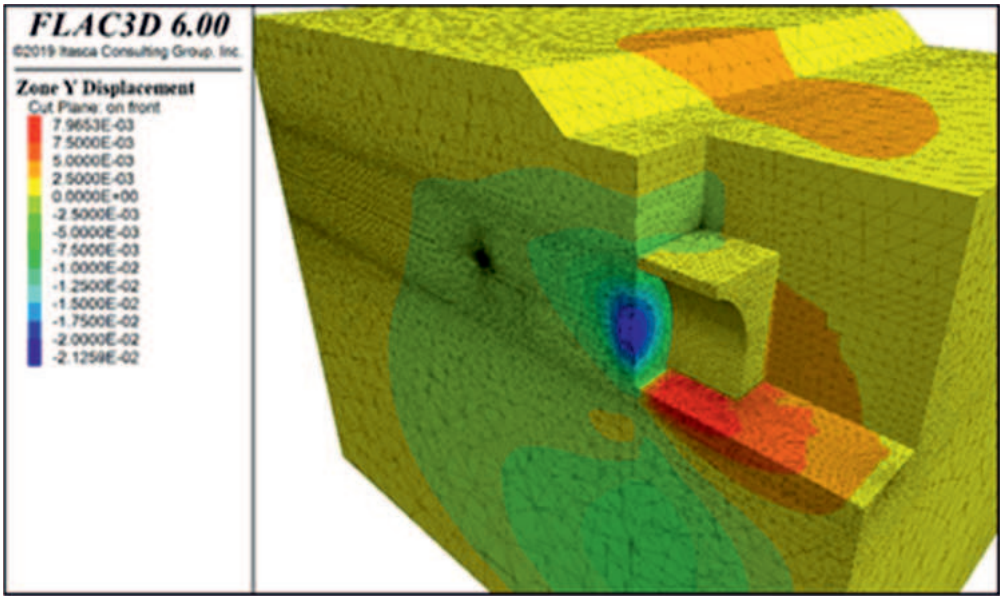

d)

Figure 14 - Displacement in the direction of the tunnel axis in FLAC^{3D}

Due to the presence of a camping beam on the top of the micro-pile, the maximum settlement at the ground surface is 1 mm, the maximum displacement in the direction of the tunnel axis is approximately 1mm, and in the final process of excavation, the displacements are going constant as shown in Fig. 15. The reason for the reversal of movements in the direction of the tunnel axis can be the creation of a backfill on the false portal.

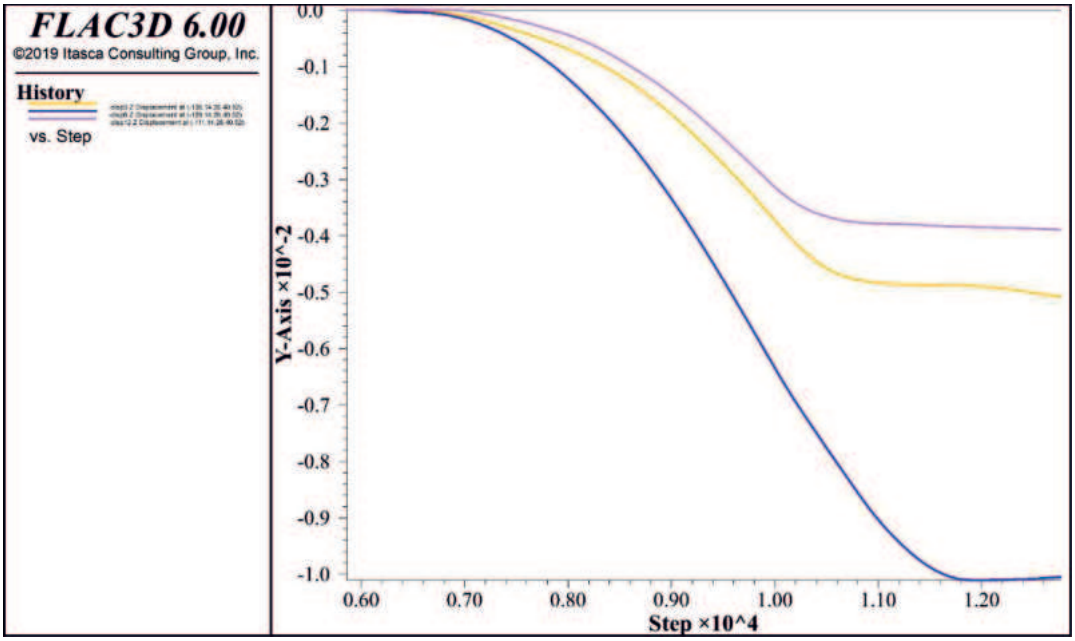

a) Z-displacement

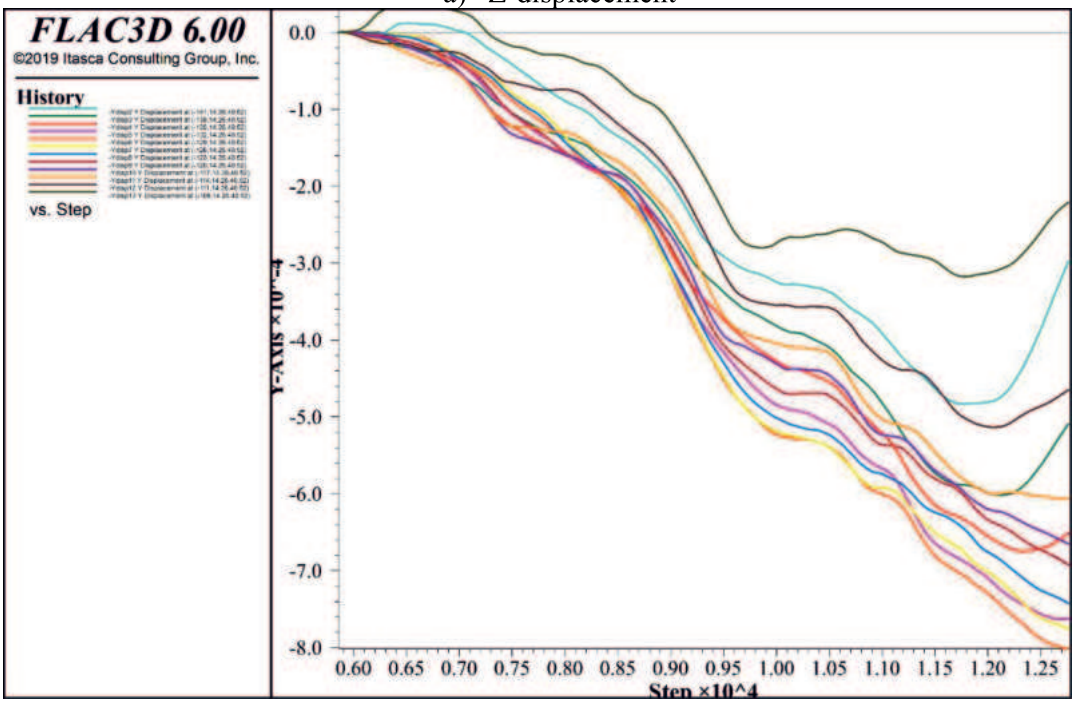

b) y-displacement

Figure 15 - History of displacement

6. MONITORING USING INCLINOMETERS

Three inclinometers were installed at the portal to observe the deformational behaviour of the ground above the tunnel at its entrance. The location and time of installation, as well as the bottom depth and measuring interval of each inclinometer are listed in Table 5.

Table 5 - Inclinometer installation details, portal 1

Inclinometer Number	Location	Initial reading date	Bottom depth (m)	Measuring interval
INC 1	Main tunnel (Right wall)	19/03/2021	14.5	0.5
INC 3	Between Main and escape tunnel	20/03/2021	18.0	0.5
INC 5	Escape tunnel left wall	19/03/2021	18.0	0.5

For the stability of the tunnel portal slope, in addition to self-stability, the effects of tunnel excavation must also be considered. By comparing the results of 3D modelling with the results of inclinometers, accuracy and numerical modelling were performed. After verifying the accuracy of numerical modelling, other outputs were examined for overall slope stability.

Inclinometer No. 1 (INC-01) is placed near the right wall of the main tunnel to record the behaviour of the slope and the effect of tunnel excavation on the stability of the slope. Inclinometer No. 1 with a length of 14.5m was installed on the right wall of the gable of the main tunnel in Portal-1. Lateral movement started on INC-01, 15-Apr-21. During the excavation of portal, RBM layers (river bed materials/sand layers) were encountered. Therefore, lateral movement was observed at a depth of 5.5 to 7m in INC-01 towards the drilling in (A-Axis). The presence of wall nails and beams in the trench limited the movement in the direction of the tunnel axis to -17cm. Numerical simulation in the alignment of the main tunnel in the transverse direction (B-Axis) showed more displacement. Figures 16 a & b show the plot of INC-01 in longitudinal and transverse directions respectively. Plots of other inclinometers are not given in the paper. However, their results are discussed below.

Inclinometer No. 3 is located between the two tunnels and in the middle of the slope portal. In addition to monitoring the slope in the middle, it is placed to study the effect of the two tunnels on each other and the tunnel-slope effect. Inclinometer No. 3, 18m long, was installed between the main tunnel and the escape tunnel in Portal-1. Lateral movement started on INC-03, 15-Apr-21. During the excavation of portal, RBM layers (river bed materials/sand layers) were encountered. Therefore, lateral movement was observed at a depth of 12.5 to 14.5m in INC-03 towards the drilling in (A-Axis). In the transverse direction of the portal (B-Axis), the amount of displacement was within the allowed range, and lateral displacement was done in both directions. While the numerical simulation shows the amount of displacement towards the escape tunnel.

Inclinometer No. 5 is placed near the left wall of the escape tunnel to record the behaviour of the slope and the effect of tunnel excavation on the stability of the slope. Inclinometer No. 5, 18m long, was installed on the upper slope of the escape tunnel in Portal-1. Movement of INC-05 was observed at 0.5 to 7m depth on 16-Jul-21 towards excavation and roadside (hill) in (A & B Axes).

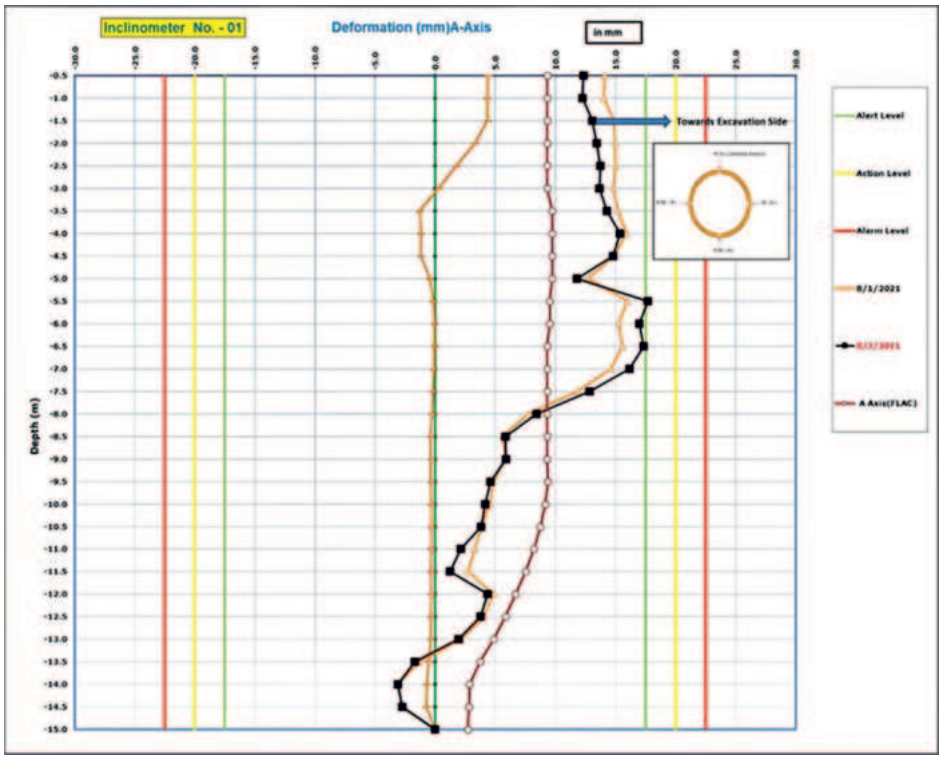

(a)

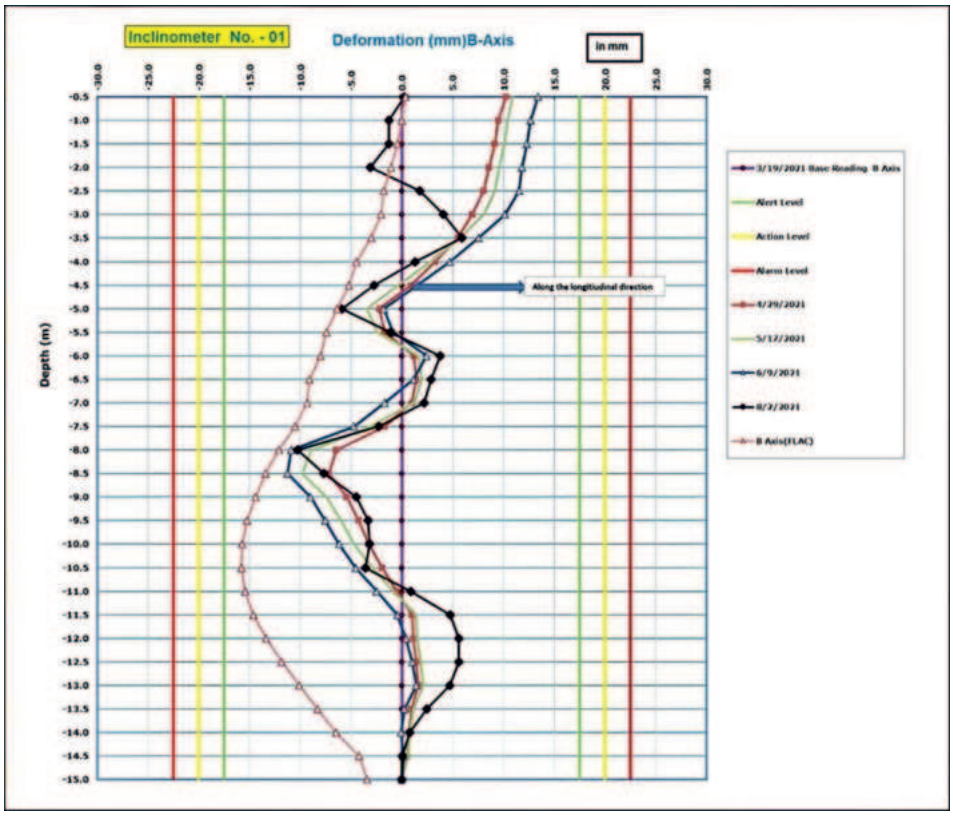

(b)

Figure 4 – Displacements recorded with an inclinometer, (a) Displacement in the longitudinal direction (INC-01), and (b) Displacement in transverse direction (INC-01)

7. CONCLUSIONS

Due to the location of the entrance opening of the tunnel in an urban location and the presence of a road above the portal, as well as the geological sensitivity of the project site, an analytical study was carried out to show the stability of the roof and support system of the portal section of the mountain tunnel in northern India. Considering the three-dimensional nature of the simulation problem, both two-dimensional and three-dimensional simulations were chosen for numerical simulation. The results of numerical simulations are:

- Injection of cement slurry around the portal was very effective in improving the ground condition and limiting the deformations.
- The integrity of micro-piles is very effective in displacements caused by drilling and preventing local soil rupture.
- By using wall beams, the amount of displacements and load on the anchors had a proper uniform distribution.
- Implementation of artificial tunnel and creation of embankment before the implementation of tunnel excavation reduces the amount of displacements and helps to improve the change of places and load on anchors.
- Simulation of the tunnel portal should be done in three dimensions due to its proximity to the ground surface and non-uniform distribution of stresses.
- Tooling is very effective for the stability of the portal strengthening and maintenance system due to its three-dimensional nature and bad geological conditions.
- The maximum settlement under the road was estimated to be 10mm. This analysis is done considering land reform (ground improvement). In addition, integration injection improves ground parameters and reduces this settlement and force in micro-pile structures.

This study also proves the importance of sensitive geological modelling, field studies, (site investigations) and their application to numerical models.

References

Chiu YC, Lee CH, Wang TT (2017). Lining crack evolution of an operational tunnel influenced by slope instability. Tunnelling and Underground Space Technology, 65:167-178.

Fabozzi S, Bilootta E (2016). Behaviour of a segmental tunnel lining under seismic actions. Procedia Engineering, 158:230-235.

Genis M (2010). Assessment of the dynamic stability of the portals of the Dorukhan tunnel using numerical analysis. Int J Rock Mech Min Sci, 47:1231-1241.

Goel R, Mitra S (2021). Weathering and its influence on rock slope stability in hilly areas. J Rock Mech Tunlg Tech (JRMTT), 27:49-62.

Goel R, Mitra S (2015). Importance of weathering in rock engineering. In: Proc of Int Conf on Engineering Geology in New Millennium, New Delhi, India, 231-245.

He Y, Sun X, Zhang M (2022). Investigation on the Deformation of Segment Linings in Cross-Fault Tunnel Considering the Creep Behavior of Surrounding Rock during Construction-Operation Period. Buildings [Online], 12.

Hu Z, Shen J, Wang Y, Guo T, Liu Z, Gao X (2021). Cracking characteristics and mechanism of entrance section in asymmetrically-load tunnel with bedded rock mass: A case study of a highway tunnel in southwest China. Engineering Failure Analysis, 122:105221.

Kaya A, Karaman K, Bulut F (2017). Geotechnical investigations and remediation design for failure of tunnel portal section: a case study in northern Turkey. Journal of Mountain Science, 14:1140-1160.

Kong C, Gao X, Cao L, Liu K (2016). Analysis of the failure of primary support of a deep-buried railway tunnel in silty clay. Engineering Failure Analysis, 66:259-273.

Lei MF, Lin DY, Yang WC, Shi CH, Peng LM, Huang J (2016). Model test to investigate failure mechanism and loading characteristics of shallow-bias tunnels with small clear distance. Journal of Central South University, 23:3312-3321.

Lei M, Peng L, Shi C (2015). Model test to investigate the failure mechanisms and lining stress characteristics of shallow buried tunnels under unsymmetrical loading. Tunnelling and Underground Space Technology, 46:64-75.

Liu G, Chen J, Xiao M, Yang Y (2018). Dynamic response simulation of lining structure for tunnel portal section under seismic load. Shock and Vibration, 2018, 7851259.

Liu X, Chen H, Liu K, He C (2017). Model test and stress distribution law of unsymmetrical loading tunnel in bedding rock mass. Arabian Journal of Geosciences, 10:184.

Shen Y, Gao B, Yang X, Tao S (2014). Seismic damage mechanism and dynamic deformation characteristic analysis of mountain tunnel after Wenchuan earthquake. Engineering Geology, 180:85-98.

Simanjuntak TDYF, Marence M, Mynett AE, Schleiss AJ (2014). Pressure tunnels in non-uniform in situ stress conditions. Tunnelling and Underground Space Technology, 42:227-236.

Tao L, Hou S, Zhao X, Qiu W, Li T, Liu C, Wang K (2015). 3-D shell analysis of structure in portal section of mountain tunnel under seismic SH wave action. Tunnelling and Underground Space Technology, 46:116-124.

Wang F, Jiang X, Niu J (2017). The large-scale shaking table model test of the shallow-bias tunnel with a small clear distance. Geotechnical and Geological Engineering, 35:1093-1110.

Wang WL, Wang TT, Su JJ, Lin CH, Seng CR, Huang TH (2001). Assessment of damage in mountain tunnels due to the Taiwan Chi-Chi Earthquake. Tunnelling and Underground Space Technology, 16:133-150.

Wang ZZ, Jiang YJ, Zhu CA, Sun TC (2015). Shaking table tests of tunnel linings in progressive states of damage. Tunnelling and Underground Space Technology, 50:109-117.

Wu D, Gao B, Shen Y, Zhou J, Chen G (2015). Damage evolution of tunnel portal during the longitudinal propagation of Rayleigh waves. Natural Hazards, 75:2519-2543.

Xiao JZ, Dai FC, Wei YQ, Min H, Xu C, Tu XB, Wang ML (2014). Cracking mechanism of secondary lining for a shallow and asymmetrically-loaded tunnel in loose deposits. Tunnelling and Underground Space Technology, 43:232-240.

Xiao JZ, Dai FC, Wei YQ, Xing YC, Cai H, Xu C (2016). Analysis of mechanical behavior in a pipe roof during excavation of a shallow bias tunnel in loose deposits. Environmental Earth Sciences, 75:293.

Xu H, Li T, Xia L, Zhao JX, Wang D (2016). Shaking table tests on seismic measures of a model mountain tunnel. Tunnelling and Underground Space Technology, 60:197-209.

Zhang J, Mei Z, Quan X (2013). Failure characteristics and influencing factors of highway tunnels damage due to the earthquake. Disaster Advances, 6:142-150.

Zhen S (2002). Contributions of returned scholars to recent economic development in Taiwan. Chinese Studies in History, 35 (3):47-51.

Zhou X, Wang J, Lin B (2014). Study on calculation of rock pressure for ultra-shallow tunnel in poor surrounding rock and its tunneling procedure. Journal of Modern Transportation, 22, 1-11.

Zhou YY, Feng XT, Xu DP, Fan QX (2017). An enhanced equivalent continuum model for layered rock mass incorporating bedding structure and stress dependence. Int J Rock Mech Min Sci, 97:75-98.